Published in final edited form as:

Mater Res Express. 2016 July ; 3(7): . doi:10.1088/2053-1591/3/7/075025.

Sodium hydroxide catalyzed monodispersed high surface area silica nanoparticles

Snehasis Bhakta[1,5], **Chandra K Dixit**[1,5], **Itti Bist**[1], **Karim Abdel Jalil**[1], **Steven L Suib**[1,2], and **James F Rusling**[1,2,3,4]

Chandra K Dixit: chandra.kumar_dixit@uconn.edu

[1]Department of Chemistry, University of Connecticut, Storrs, CT 06269-3060, USA [2]Institute of Materials Science, University of Connecticut, Storrs, CT 06269-3136, USA [3]Department of Cell Biology, University of Connecticut Health Center, Farmington, CT 06030, USA [4]School of Chemistry, National University of Ireland at Galway, Galway, Ireland

Abstract

Understanding of the synthesis kinetics and our ability to modulate medium conditions allowed us to generate nanoparticles via an ultra-fast process. The synthesis medium is kept quite simple with tetraethyl orthosilicate (TEOS) as precursor and 50% ethanol and sodium hydroxide catalyst. Synthesis is performed under gentle conditions at 20 °C for 20 min Long synthesis time and catalyst-associated drawbacks are most crucial in silica nanoparticle synthesis. We have addressed both these bottlenecks by replacing the conventional Stober catalyst, ammonium hydroxide, with sodium hydroxide. We have reduced the overall synthesis time from 20 to 1/3 h, ~60-fold decrease, and obtained highly monodispersed nanoparticles with 5-fold higher surface area than Stober particles. We have demonstrated that the developed NPs with ~3-fold higher silane can be used as efficient probes for biosensor applications.

Keywords

sodium hydroxide; silica nanoparticle; Stober; silanization; high surface area

Introduction

Silica nanoparticles (SiNPs) constitute an important fraction of research and product development. The applications of SiNPs range from biosensors to drug-delivery vehicles [1–5]. Therefore, a fine-tuning of NP properties is sought. These physico-chemical properties

[5]Authors contributed equally

Supplementary material for this article is available online

Author contribution

SB and CKD have conceived the idea. SB, IB, CKD, and KAJ have contributed to the process development and optimization. CKD, JFR, and SLS have mentored the work and contributed intellectually. SB, IB, KAJ, CKD, JFR, and SLS have performed data analysis along with writing the manuscript.

Conflict of interest

Authors claim no conflict of interest for this work.

include surface charge, colloidal dispersivity, surface roughness, and better functional-customization [6, 7]. These properties are reliant on the size and morphology of NPs. SiNPs are synthesized mainly by base-catalyzed nucleation of precursor silanes in colloids, reverse microemulsions, chemical vapor condensation, and other methods, which are summarized in supplementary table 1 along with their advantages and disadvantages. Colloidal synthesis using ammonium hydroxide (NH_4OH) as a catalyst is by far the most common method for making SiNP due to the advantage of manipulating reaction conditions and parameters to achieve desired NP sizes and shapes [8, 9]. However, the inherent drawbacks of these methods are high polydispersity and the requirement of excessive washing to remove ammonia from the sample [10], which we also have observed during our experiments. There are several modifications performed on the basic Stober approach for NP synthesis, which included mainly using cationic aminoacids, organic ligands, variable alkoxy chain-length silanes [11–15]. These methods enabled rapid synthesis with more control on the size and shape manipulation of such NPs. However, reverse microemulsion approaches provide high degree of monodispersity comparative to the modified Stober methods by allowing a controlled formation of nanoparticles within the micellar cores. The sizes of micelles can be controlled by adjusting the ratio of surfactant to polar solvent which will eventually govern the amount of reactant entrapped, and thus the size of the nanoparticle [16]. Extensive post-processing for removing the surfactants from the synthesis medium makes microemulsion approaches relatively expensive. Industrially, SiNPs are prepared as powder by gas-phase methods. This approach is relatively faster to create NPs as compared to wet methods, with at least a 3-fold higher magnitude of diffusion and thus faster reaction times. Controlling the size and morphology of NPs is challenging with this approach in addition to the higher tendency of aggregation of particles during synthesis [12]. The instrumentation itself is also very costly and requires technical expertize [17]. Also, this approach presents a health hazard where workers are exposed to the nano-powders synthesized by this process. Microwave-assisted SiNP synthesis has been reported for fast synthesis within minutes [18]. This approach can be industrially favorable but the restrictions outweigh the advantages. The restrictions of microwave method include mainly costly instrumentation [19], high operating cost, expertize required for operation, and strong dependence of particle morphology on the microwave energy that may cause wrong nanoparticle size with a slight change in the introduced energy. In addition, extensive optimization is required to understand this dependence of microwave energy and nanoparticle size [20]. Also, it poses a health hazard if the operator is exposed to microwave [21].

Therefore, even with a wider size distribution obtained with sol–gel synthesis process, it is still a preferable method due to its simplicity which allows for the manipulation of reaction parameters to achieve control of the size and morphology simply by adjusting the reaction parameters. In this process, SiNPs are formed by hydrolysis and condensation of silicon alkoxides, such as tetraethyl orthosilicates (TEOS), in the presence of mild acids (hydrochloric acid) or base (ammonium hydroxide). A plausible reaction mechanism is depicted in figure 1. Base-catalyzed condensation-mediated synthesis is very fast in comparison to the acid-catalyzed reaction because latter proceeds through hydrolysis and requires an additional step of condensation for nucleating.

The main challenges of the classical colloidal synthesis of SiNP that we have addressed in this report are (i) longer reaction times ~20 h, and (ii) use of NH_4OH as a catalyst, which being volatile may not provide appropriate nucleation resulting in polydispersed particles [22–24]. Stober in his original report (1968) claimed to have achieved completion of particle formation within 15 min only for few instances but his method advocated to perform polymerization for at least 2 h [25]. However, later reports have employed several reaction times but 2 h [26, 27]. Ammonia released by the decomposition of NH_4OH during the synthesis may also either get entrapped in the material or get adsorbed to the surface of the particle thus interfering with the analysis and further processing [10, 28]. We have replaced NH_4OH with sodium hydroxide (NaOH) as a catalyst. Dingsoyr and Christy (2000) in a seminal work has described NaOH as potential base catalyst [29]. They have employed a multiparametric mathematical regression modeling approach to perform design of experiment for exploring the SiNP synthesis. We have employed NaOH as the catalyst for our study with a completely different approach where focus was mainly kept at the experimental understanding of the methodology rather than the theoretical modeling. Recently, Hyde and colleagues has employed NaOH for synthesis but they have directed their work on a two-step approach based on an acid-catalysed hydrolysis followed by NaOH-catalysed condensation [30]. Addition of the hydrolysis approach complicates the whole procedure itself with increased synthesis time.

In the current work replacing NH_4OH with NaOH has allowed us to reduce synthesis time from ~20 to ~1/3 h (a 60-fold reduction), and this has tremendously increased the surface area (~5-folds increase) enabling us to significantly increase the amount of grafted functional groups (3-fold increase). In addition, stable and highly monodispersed SiNPs in a size range of 60–550 nm were obtained. In addition, our approach has covered all the aspects of an optimized process development, which were lacking in similar previous studies by Dingsoyr [29] and Hyde [30]. The work described in this report has tremendous potential as being adapted for industrial synthesis after scaling up. In addition, the NPs synthesized via this route are of superior quality and may have extensive use in disease diagnostics, therapeutics, and *in vivo* imaging.

Experimental

Chemicals and materials

Tetraethylorthosilicate (TEOS, ≥99%), (3-aminopropyl)-triethoxysilane (APTES, ≥98%), ethanol (200 proof), ammonium hydroxide, sodium hydroxide, ninhydrin, sodium phosphate dibasic and sodium phosphate monobasic were from Sigma-Aldrich. The silica wafer for scanning electron microscopy (SEM) was from Ted Pella, Inc. All solutions were prepared in 18 MΩ cm deionized water (DIW). All the prepared solutions were filtered using 0.45 μm filters (Fisher) prior to use. Phosphate buffer (10 mM, pH 7.3) was employed for the experiments until stated otherwise.

Instrumentation

SEM was performed with the Teneo LVSEM. Hydrodynamic size of NPs was measured with dynamic light scattering (DLS) using ALV/CGS-3 instrument. Zeta potential of NP colloid

was analyzed with ZetaPlus analyzer (Brookhaven Instruments Corp.). Nitrogen adsorption-based Brunauer–Emmett–Teller (BET) analysis was performed with Quantchrome autosorb iQ2.

Synthesis of SiNPs

TEOS was catalyzed with NaOH in a basic ethanol–water medium for 20 min and NPs were developed as a result of condensation reactions. A set of NH_4OH-catalyzed classical SiNP synthesis was also performed for comparative studies. Optimization of the process was performed for determining the ratio of ethanol to water in the reaction medium, concentration of TEOS, and NaOH concentration (details in SI).

Ethanol–water ratio in the synthesis medium was optimized; a stock solution of NaOH (1 M) prepared in DIW was added to TEOS (90 mM) prepared in different solvent compositions. TEOS was optimized for a concentration range of 10–120 mM, such that TEOS was directly added to the optimized ethanol–water solvent spiked with 20 mM NaOH to obtain the desired concentration. Furthermore, NaOH was optimized using varying concentrations between 10 mM to 20 mM in order to analyze the effect of catalyst on NP size and shape. During optimization, TEOS was slowly added to each set of NaOH concentration in order to obtain final TEOS concentration. The reaction was allowed to stir for 20 min at 600 rpm. Later, the SiNPs were centrifuged and washed twice each with ethanol and DIW. Finally, the nanoparticles were stored in DIW at room temperature for further studies. Stober-NPs were synthesized according to a previously described method SI figure 4) [31].

SEM analysis

NPs were concentrated and re-suspended in ethanol. Later, colloid was drop coated on a silica wafer and was allowed to dry overnight at room temperature. The dried sample was coated with a ~10 nm thick gold layer using chemical vapor deposition system. The prepared samples were loaded into a Teneo LVSEM and were imaged.

Analysis of surface

Surface of the nanoparticles was characterized in terms of (a) surface area, and (b) silane loading efficiency. Nitrogen adsorption-based BET analysis was performed for ‘a’ using SiNPs (with a diameter ~550 nm) and comparatively sized Stober-NP (~600 nm). For ‘(b)’, the developed SiNPs and Stober-NP were functionalized with 3-aminopropyltriethoxy silane and the number of grafted amines was quantified for analysis. At first, the optimum silane concentration for functionalization of Stober-NPs was obtained by incubating those with different concentrations of APTES (45, 90, 180, 270 mM) for 3 h in a 95% ethanol medium. Later, quantification of amino groups on the functionalized NPs was performed with ninhydrin (100 μl, 20 mg ml^{-1}). At the optimum silane concentration, APTES was grafted on 10 mg each of the developed SiNPs and Stober-NPs in 95% ethanol followed by ninhydrin-based amino group quantification. A standard curve for APTES was generated with ninhydrin tests using concentrations of 1 mM, 100 μM, 10 μM, 1 μM, 100 nM, 10 nM, 1 nM.

Analysis of ammonia in the cleaned NP system

Ninhydrin reacts with amines via a series of reactions [32] as illustrated in reactions 1–2

$$\text{Ninhydrin} + \text{R}-\text{NH}_2 \rightarrow \text{Partially reduced ninhydrin } (1,3-\text{diketohydrindol}) + \text{NH}_3. \quad (1)$$

$$\text{Ninhydrin} + \text{NH}_3 + \text{Partially reduced ninhydrin} \rightarrow \text{Blue}-\text{purple colored pigment}. \quad (2)$$

As obvious that ammonia is a key component in the ninhydrin reaction therefore, we have speculated that if Stober-NPs even after several washes generate a blue-purple color, as depicted in SI figure 1, then the ammonia may be present in the system with a high probability of being adsorbed on the NP surface. Further studies for confirmation of ammonia adsorbed to the particle surface are required. Other reports have also described the reaction of ninhydrin with pure ammonia [33] and have contributed to the development of this hypothesis.

Results and discussion

We have employed sodium hydroxide, a common shelf-reagent, as an alternative catalyst for ammonium hydroxide for synthesizing SiNP. Sodium hydroxide served as a better catalyst for this condensation reaction, as also described by Dingsoyr and Christy in their regression modeling approach [29], because (i) unlike ammonium hydroxide, which has a tendency to adsorb on the NP surface (figure 2) [28], it is easy to remove NaOH from the reaction mixture, as confirmed by the ninhydrin test (ii) the abrasive properties of NaOH provided a higher surface area, as confirmed by the surface area analysis using N_2 gas adsorption-based BET method, and (iii) the reaction with NaOH completed in 20 min compared to 20 h with NH_4OH. Therefore, the developed approach for SiNP synthesis is time saving and does not involve intensive post processing to remove by-products and reagents.

The whole process was optimized for several parameters; however, most important are the solvent ratio in reaction medium (supplementary table 2), TEOS concentration (supplementary table 3), and NaOH concentrations (supplementary table 4). Reaction medium plays a crucial role in nanoparticle synthesis. As observed in this study (supplementary table 2), solvent that is predominant in the medium has conclusive effects [34]. Single solvent systems are usually preferred because that minimizes the requirement of careful selection of co-reactants according to their solubility, reactivity, and other parameters. However, co-solvent schemes are always sought as they facilitate many new physical processes to occur. Pure ethanol in comparison to pure water has higher solubility of TEOS and therefore is a suitable solvent for synthesis but the hydrolysis rate of TEOS in pure ethanol is very slow [35]. After adding water to pure ethanol, the reaction kinetics change significantly, as evident from supplementary table 1. In silica NP synthesis, the core of the reaction is governed by two components as illustrated in figure 1; (i) effective hydrolysis, and (ii) enhanced condensation reaction to take place. Silanes are highly susceptible to hydrolysis in the presence of water while they condense effectively in ethanol

medium [36]. In addition, on the contrary to an acid-catalyzed reaction, a base-catalyzed reaction mainly proceeds through condensation (figure 1) [37, 38]. The acid-catalyzed reaction is a 2-step process taking place through hydrolysis followed by condensation. Thus, a base-catalyzed reaction is faster than acid catalysis.

Therefore, based on this theory we have opted for a base catalyzed synthesis. An appropriate ratio of water to ethanol was also sought for fast NP synthesis. We have optimized several ratios of DIW and ethanol (supplementary table 2) and found that the fastest NP synthesis is obtained with equivalent DIW and ethanol volumes (1:1) that will effectively provide the fastest hydrolysis and condensation in tandem. However, typical ratio for DIW-ethanol used in Stober and modified Stober methods are 1:19 (volumetric) [31]. Under similar conditions, NaOH-catalyzed reaction was faster than the NH_4OH catalysis. Although, NH_4OH can serve as a better source for hydroxyls for longer durations than NaOH due to its partial ionization and its ability to recycle between NH_3 and NH_4^+ states in an aqueous solution as speculated in previous reports [29, 39]. On the contrary, we anticipate that NaOH being a stronger base than NH_4OH has the highest ionizability and thus completely dissociates to ions. The higher number of ions provided by an equimolar solution of NaOH in comparison to NH_4OH significantly enhances the condensation reaction and thus the SiNP formation. At the same time, ammonia gas generated due to NH_4OH degradation has a higher tendency to get adsorbed on the surface of the particles being generated that will have impact on the applications of the particles developed (figure 2) [40].

NaOH is known to have strong abrasive properties. Such type of base-etching is commonly employed for increasing the surface area of metallic compositions including planar metal surfaces [41] and metallic nanoparticles [42]. Therefore, we have also employed NaOH as a replacement to conventionally used ammonium hydroxide as base catalyst for NP synthesis (figure 3). We have obtained a BET surface area of ~117 $m^2\ g^{-1}$ with pore diameter of ~2 nm for NaOH SiNP. For Stober-NP surface area and pore size were ~22 $m^2\ g^{-1}$ and ~6 nm, respectively. Thus, we have observed practically a 5 fold higher surface area. This increase in surface area was used to our benefit to load silane on the NP surface for demonstrating its applicability (figure 4, SI figure 3, SI figure 5). This significant increase in surface area of the synthesized SiNPs with higher number of grafted functional groups will lead to higher biomolecule loading capacity per SiNP and thus these will contribute towards the development of a better chromatography matrix, high sensitivity immunoassays, and other.

The developed method, in comparison to Stober-NP, provides better surface properties, such as higher surface area and higher functional group loading capacity. In addition, as per the Material Safety guidelines, the NaOH catalyst is extremely safer than NH_4OH, which can decompose to hazardous nitrogen oxides and ammonia under variable conditions. We have developed different particle sizes by manipulating sodium hydroxide concentrations in the reaction mixture. Depending on the NaOH concentration, particle sizes were between 60 and 550 nm in diameter (table 1, figure 2, SI figure 1). The DLS measurements corroborated with the SEM results (SI figure 2). Zeta-potentials for the particles were in the range of −35 to −45 mV, which is in agreement with the charge-dependent colloidal stability. Our findings agree to the notion of catalyst-mediated reaction as we reported a sharp increase in the particle size with a slight increase in NaOH concentration. However, these are contradictory

to a previous report employing NaOH as catalyst for their study employing mathematical modeling for understanding the particle synthesis mechanism. SiNPs were found by their group to decrease in size with an increase in the NaOH concentration. On the contrary, we recorded an increase in the particle size with increasing NaOH concentration and a very fast gelation after the NaOH range mentioned in table 1.

Microwave-mediated SiNP synthesis has been previously reported for quick NP preparation within minutes [18, 43]. It is faster than even to our developed method; however, the drawbacks of microwave method outweighs the advantage of fast synthesis. The potential bottlenecks of microwave synthesis including the continuous microwave reactor-based method extends from health hazard due to microwave exposure to high manufacturing cost due to excessive energy consumption, but the most important is the poor control over nanoparticle size and morphology of the synthesized particles [20, 21]. The developed method allows for the synthesis of a wide NP size range, while the microwave-assisted approach only allows for small size range, viz 5–250 nm.

Conclusions

As a general rule, the catalyst employed has a significant impact on the nature of the product. This generalization stand correct in case of nanoparticle synthesis as well where particle properties completely changed by replacing NH_4OH with NaOH in the conventional Stober method of SiNP synthesis. We were able to reduce the synthesis time by ~60-fold from 20 to 1/3 h. We obtained particles that have ~5-fold more surface area (117 $m^2\ g^{-1}$) compared to Stober-NPs (22 $m^2\ g^{-1}$). We will employ the developed SiNPs with inherently increased surface area for bio-detection, electrochemistry, and immunolabelling. However, their application can be extended and used for a plethora of applications including catalysis, chromatography, and solar cells.

Supplementary Material

Refer to Web version on PubMed Central for supplementary material.

Acknowledgments

Authors acknowledge the financial support from the Green Emulsions, Micelles, and Surfactants Center (GEMS) at University of Connecticut and grants EB016707 and EB014586 from the National Institute of Biomedical Imaging and Bioengineering (NIBIB), NIH, USA for financial support of this work. Authors acknowledge FEI UCONN (University of Connecticut) for their microscopy facilities. SB would like to thank the FEI UCONN for a fellowship grant. Authors would like to thank Biswanath Dutta in SLS Lab for his valuable discussions on BET analysis. SLS acknowledges support of the US Department of Energy, Basic Energy Sciences, Division of Chemical, Geological and Biological Science under grant DE-FGO2-86ER13622.A000.

References

1. Bhakta S, Seraji MSI, Suib SL, Rusling JF. ACS Appl. Mater. Interfaces. 2015; 7:28197–28206. [PubMed: 26636440]
2. Biswas S, Poyraz AS, Meng Y, Kuo C-H, Guild C, Tripp H, Suib SL. Appl. Catal. B. 2015; 165:731–741.
3. Poyraz AS, Kuo C-H, Biswas S, King'ondu CK, Suib SL. Nat. Commun. 2013; 4:2952. [PubMed: 24335918]

4. Roy S, Dixit CK, Woolley R, O'Kennedy R, McDonagh C. Langmuir. 2012; 28:8244–8250. [PubMed: 22568772]
5. Roy S, Dixit CK, Woolley R, O'Kennedy R, McDonagh C. Nanotechnology. 2012; 23:325603. [PubMed: 22825430]
6. Dixit CK, Roy S, Byrne C, O'Kennedy R, McDonagh C. Analyst. 2013; 138:6277. [PubMed: 24010130]
7. Roy S, Korzeniowska B, Dixit CK, Manickam G, Daniels S, McDonagh C. J. Nanomater. 2015; 2015:e761517.
8. Huang Y, Pemberton JE. Colloids Surf. A. 2010; 360:175–183.
9. Kumar A, Sevonkaev I, Goia DV. J. Colloid Interface Sci. 2014; 416:119–123. [PubMed: 24370410]
10. Pan G-H, Barras A, Boussekey L, Addad A, Boukherroub R. J. Mater. Chem. C. 2013; 1:5261–5271.
11. Patwardhan SV, Clarson SJ. Mater. Sci. Eng. C. 2003; 23:495–499.
12. Nozawa K, Gailhanou H, Raison L, Panizza P, Ushiki H, Sellier E, Delville JP, Delville MH. Langmuir. 2005; 21:1516–1523. [PubMed: 15697302]
13. Patwardhan SV, Emami FS, Berry RJ, Jones SE, Naik RR, Deschaume O, Heinz H, Perry CC. J. Am. Chem. Soc. 2012; 134:6244–6256. [PubMed: 22435500]
14. Masalov VM, Sukhinina NS, Kudrenko EA, Emelchenko GA. Nanotechnology. 2011; 22:275718. [PubMed: 21613739]
15. Chen S-L, Dong P, Yang G-H, Yang J-J. Ind. Eng. Chem. Res. 1996; 35:4487–4493.
16. Woolley R, Roy S, Prendergast Ú, Panzera A, Basabe-Desmonts L, Kenny D, McDonagh C. Nanomed. Nanotechnol. Biol. Med. 2013; 9:540–549.
17. Feng J, Biskos G, Schmidt-Ott A. Sci. Rep. 2015; 5:15788. [PubMed: 26511290]
18. Lovingood DD, Owens JR, Seeber M, Kornev KG, Luzinov I. ACS Appl. Mater. Interfaces. 2012; 4:6875–6883. [PubMed: 23182127]
19. Kappe CO, Dallinger D. Nat. Rev. Drug Discovery. 2006; 5:51–63. [PubMed: 16374514]
20. Umer A, Naveed S, Ramzan N, Rafique MS. Nano. 2012; 07:1230005.
21. Bilecka I, Niederberger M. Nanoscale. 2010; 2:1358. [PubMed: 20845524]
22. Lei Z, Xiao Y, Dang L, Lu M, You W. Microporous Mesoporous Mater. 2006; 96:127–134.
23. Lindberg R, Sundholm G, Pettersen B, Sjöblom J, Friberg SE. Colloids Surf. A. 1997; 123–124:549–560.
24. Lindberg R, Sjöblom J, Sundholm G. Colloids Surf. A. 1995; 99:79–88.
25. Stöber W, Fink A, Bohn E. J. Colloid Interface Sci. 1968; 26:62–69.
26. Bogush GH, Tracy MA, Zukoski CF. J. Non-Cryst. Solids. 1988; 104:95–106.
27. Tadanaga K, Morita K, Mori K, Tatsumisago M. J. Sol-Gel Sci. Technol. 2013; 68:341–345.
28. Roque-Malherbe R, Marquez-Linares F, Del Valle W, Thommes M. J. Nanosci. Nanotechnol. 2008; 8:5993–6002. [PubMed: 19198337]
29. Dingsøyr, E.; Christy, AA. Surface and Colloid Science. Razumas, PV., et al., editors. Springer: Berlin; 2000. p. 67-73.
30. Hyde EDE, Moreno-Atanasio R, Millner PA, Neville F. J. Phys. Chem. B. 2015; 119:1726–1735. [PubMed: 25543459]
31. Ibrahim IAM, Zikry AAF, Sharaf AF. J. Am. Sci. 2010; 6:985–989.
32. Harding VJ, MacLean RM. J. Biol. Chem. 1916; 24:503–517.
33. Friedman M. J. Agric. Food Chem. 2004; 52:385–406. [PubMed: 14759124]
34. Jiang X, Wang Y, Li M. Sci. Rep. 2014; 4:6070. [PubMed: 25317902]
35. Jang KW, Choi SH, Pyun SI, John MS. Mol. Simul. 2001; 27:1–16.
36. Brinker CJ. J. Non-Cryst. Solids. 1988; 100:31–50.
37. Arkles, B.; Steinmetz, JR.; Zazyczny, J.; Mehta, P. Silanes and Other Coupling Agents. Vol. 1. Utrecht/Boca Raton, FL: VSP/CRC Press; 1992. p. 91-104.
38. Berendjchi A, Khajavi R, Yazdanshenas M-E. Iran J. Org. Chem. 2013; 5:1079–1083.
39. Fu C-F, Tian SX. J. Phys. Chem. C. 2013; 117:13011–13020.

40. Leewis CM, Kessels WMM, van de Sanden MCM, Niemantsverdriet JW. Appl. Surf. Sci. 2006; 253:572–580.
41. Yasuda K, Saito R. IOP Conf. Ser.: Mater. Sci. Eng. 2014; 61:012007.
42. Eid KA, Azzazy HM. Int. J. Nanomed. 2012; 7:1543–1550.
43. Lovingood DD, Owens JR, Seeber M, Kornev KG, Luzinov I. J. Vis. Exp. 2013; 82:51022.

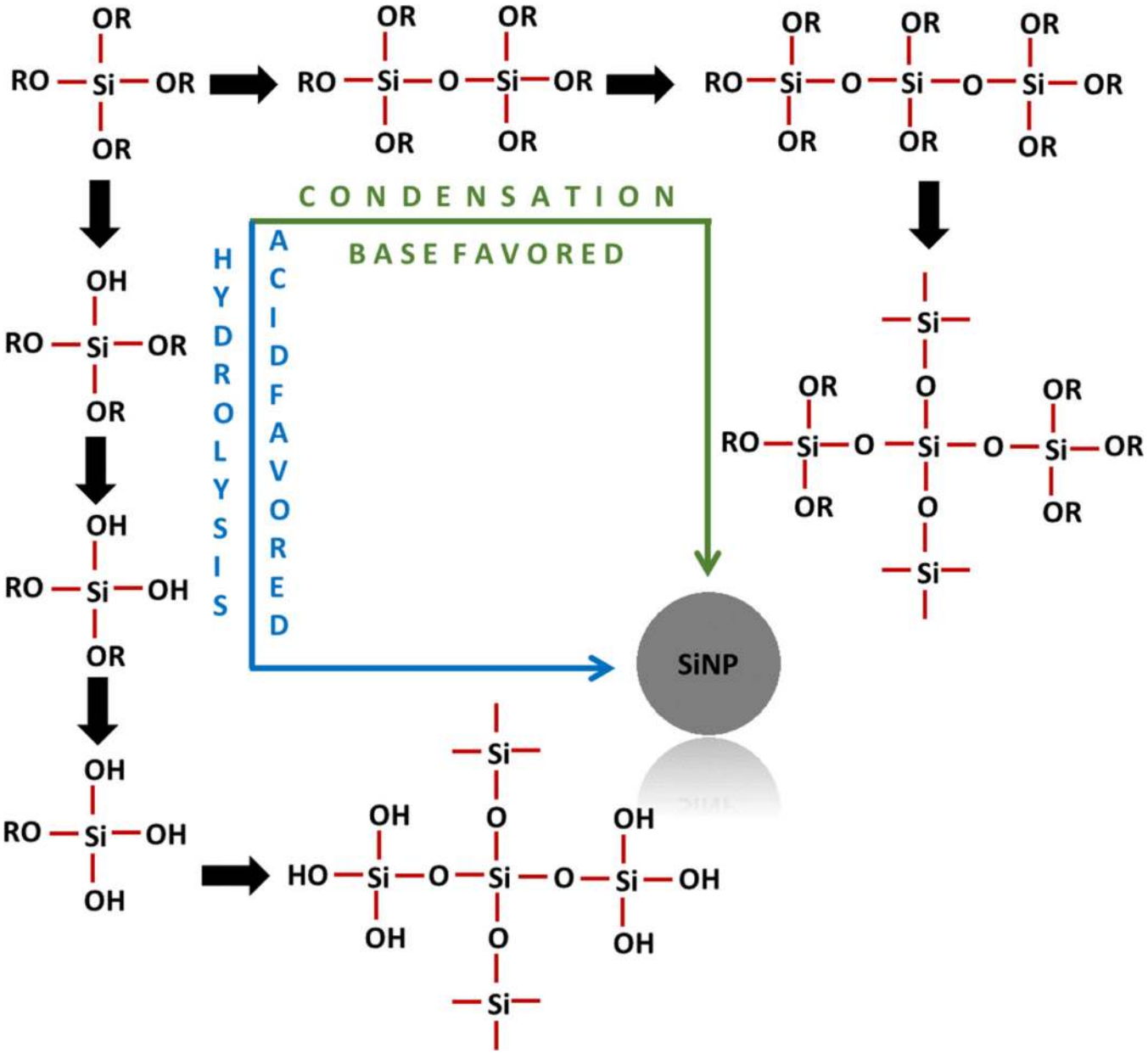

Figure 1.

Mechanism of nucleation of silica precursor to form NPs. Silica precursor can approach nucleation either via condensation or through hydrolysis followed by condensation. Condensation nucleation is typically followed under mild to extreme basic conditions where reaction has no silanol intermediates formed. Conversely, hydrolysis is mostly favored under mild to strong acidic conditions where the system has a higher tendency to form silanols. Later, hydrolysis products of silanols condense to form NPs. Therefore, the base-assisted condensation accelerates the NP synthesis in comparison to acidic conditions.

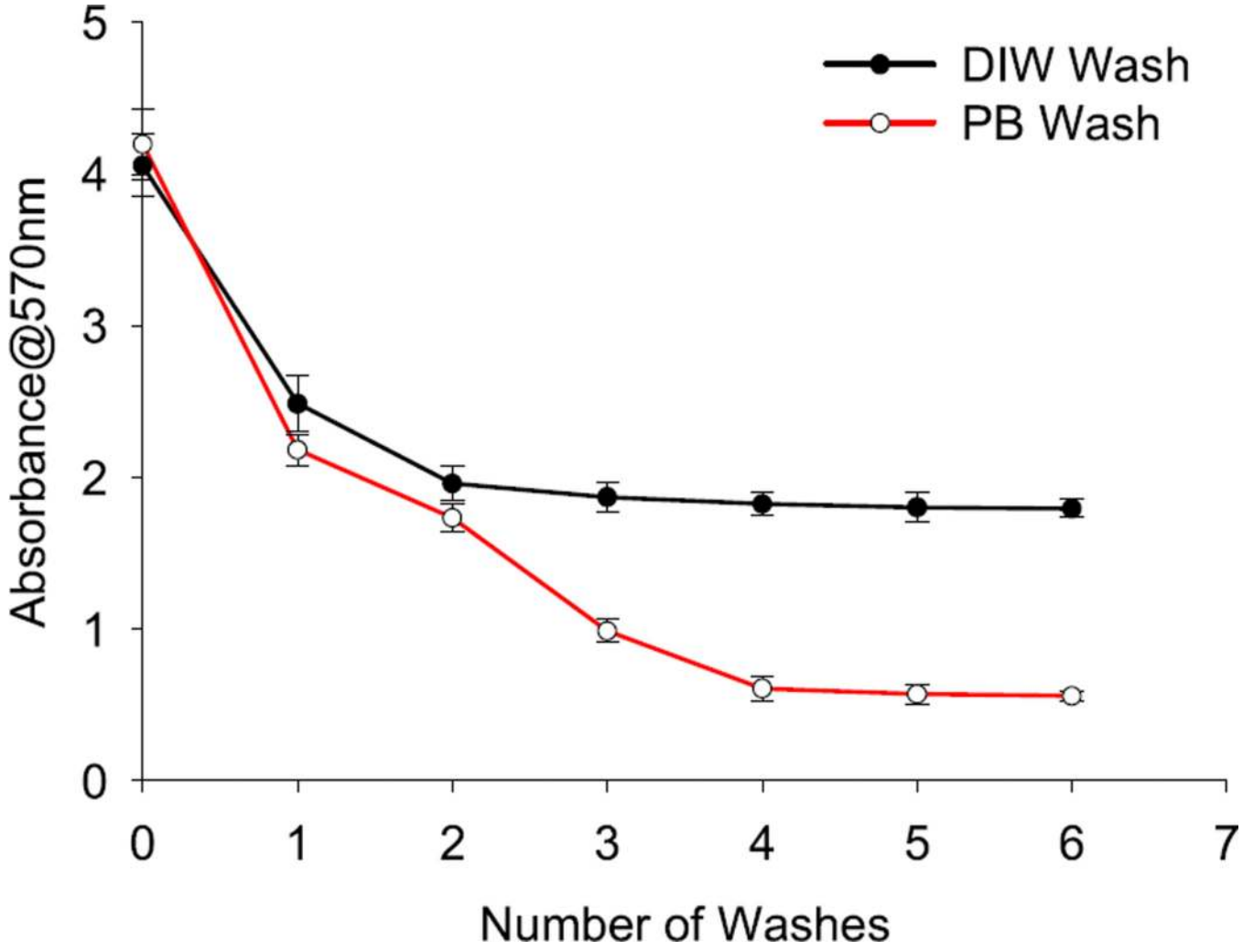

Figure 2.

Illustration of the presence of ammonia in the Stober-NP system and effect of subsequent washings with DIW and phosphate buffer (PB). At each step 50 μl sample was withdrawn and centrifuged to remove solvent. Each sample set was then incubated with 100 μl ninhydrin (20 mg ml^{-1}) at 100 °C in a thermostat for 10 min absorbance was measured at 570 nm wavelength against ethanol blank. Error bars are standard deviation from the mean of each data point.

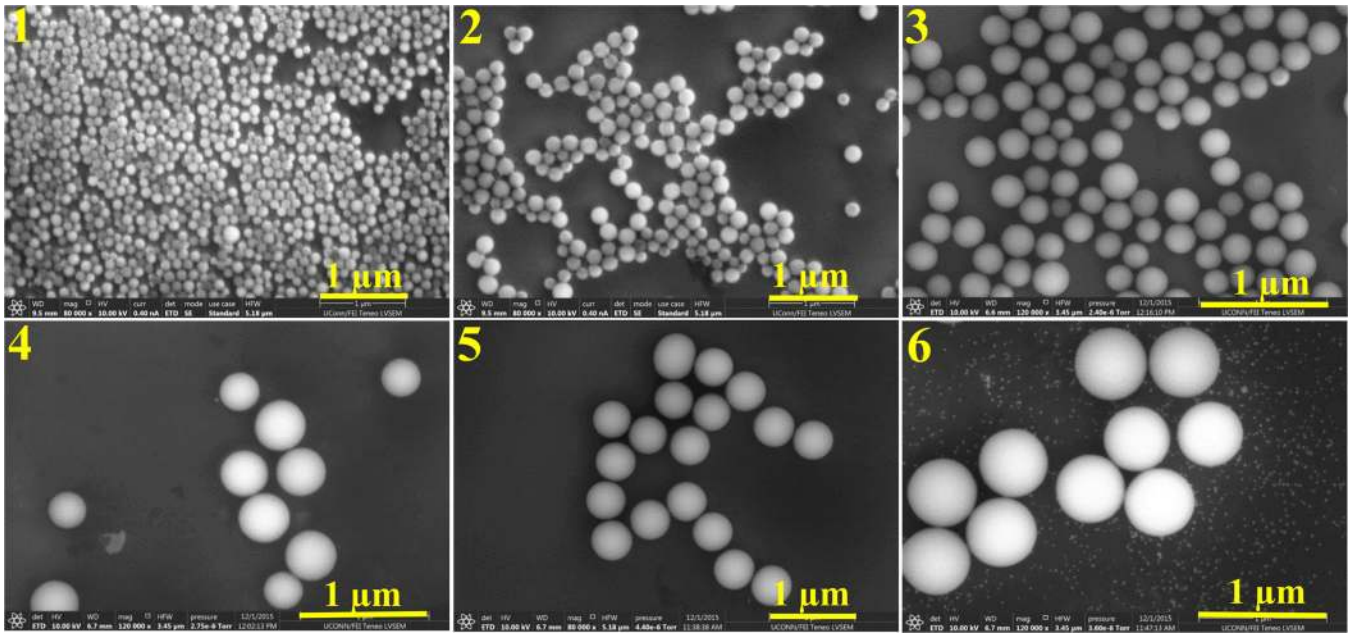

Figure 3.

SEM images of SiNPs prepared under different NaOH formulations described in table 1. Particle diameters were in the range of 50–550 nm.

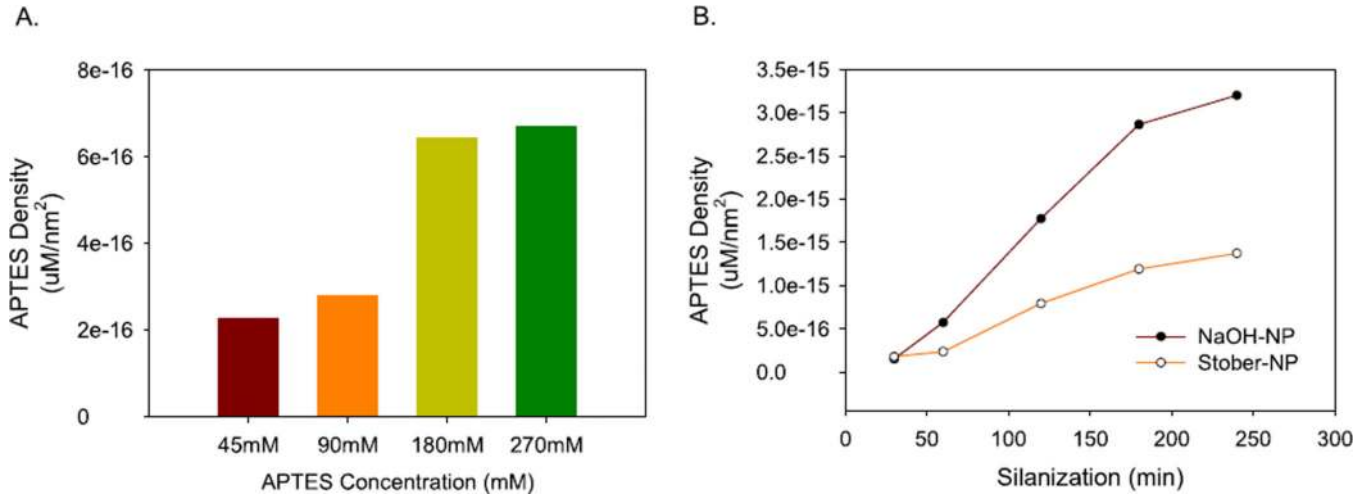

Figure 4.

Silanization of developed SiNP (550 nm) and Stober-NPs (600 nm) using APTES. (A) At first, the silanization process was optimized for APTES concentrations (45, 90, 180, and 270 mM) using 600 nm Stober-NPs. Silanization was performed in 95% ethanol for 3 h. (B) Based on the optimum APTES concentration density, as obtained from '(A)', 180 mM solution was employed for silanization of the developed SiNP and Stober-NP using the previously stated conditions over a time period of four hours. APTES concentration density was calculated as the ratio of representative concentration of APTES obtained from standard calibrator (Supplementary figure 3) for per particle to the surface area of the particle (refer to supplementary information for details).

Table 1

Physical properties of different silica nanoparticle from different NaOH formulations[a].

Concentration of NaOH (mM)	FESEM size (nm)	Hydrodynamic radius(nm)	Zeta-potential (mV)
10 (sample 1)	60(±2.4)	49(±1.2)	−45.2 (±5)
12 (sample 2)	85(±3.1)	68(±1.9)	−36.1(±3)
14 (sample 3)	290(±12.3)	148(±1.8)	−36.3(±1)
16 (sample 4)	380(±13.1)	197(±9.5)	−40.2(±1)
18 (sample 5)	490(±22.1)	255(±7.8)	−38.4(±2)
20 (sample 6)	550(±22.5)	286(±9.9)	−35.5(±1)
25	Gel		

[a]Tetraethylorthosilicate concentration was 90 mM and 1:1 water–ethanol was employed as medium for synthesis; pH for the measurements was 6.8 with DIW as medium.